A finite element method for surface restoration with smooth boundary conditions

U. Clarenz, U. Diewald, G. Dziuk, M. Rumpf, R. Rusu

Abstract

In surface restoration usually a damaged region of a surface has to be replaced by a surface patch which restores the region in a suitable way. In particular one aims for C^1-continuity at the patch boundary. The Willmore energy is considered to measure fairness and to allow appropriate boundary conditions to ensure continuity of the normal field. The corresponding L^2-gradient flow as the actual restoration process leads to a system of fourth order partial differential equations, which can also be written as system of two coupled second order equations. As it is well–known, fourth order problems require an implicit time discretization. Here a semi–implicit approach is presented which allows large timesteps. For the discretization of the boundary condition, two different numerical methods are introduced. Finally, we show applications to different surface restoration problems.

AMS-Classification: 35K35, 65M60, 68U07, 68U10, 74K25

1 Introduction

In this paper we will discuss surface restoration and surface blending based on Willmore flow with boundary conditions. This approach is in general not new. Several methods based on the same or similar ideas can be found in the literature [24, 25, 29]. Our contribution is to give a proper weak formulation of the corresponding initial and boundary value problem, to discretize this in space consistently using a finite element scheme on triangular grids, and in time applying a semi–implicit backward Euler discretization. The resulting algorithm is easy to implement, it allows for large time steps, and behaves robustly in the application. The method presented here is founded upon the corresponding approach [23] for surfaces without boundary. Here, we will derive from this approach appropriate discretization schemes for Willmore flow problems with boundary conditions.

Let us consider the following problem. Suppose a two-dimensional surface $\tilde{\mathcal{M}}^0$ embedded in $\mathbb{R}^3$ is given and a subset $\mathcal{M}^0 \subset \tilde{\mathcal{M}}^0$ is in bad shape. Either $\mathcal{M}^0$ is a destroyed region on the surface $\tilde{\mathcal{M}}^0$, where the remaining surface $\mathcal{M}^{ext} := \tilde{\mathcal{M}}^0 \setminus \mathcal{M}^0$ is in good condition, or $\mathcal{M}^0$ is an initial blending surface closing a given surface $\mathcal{M}^{ext} := \tilde{\mathcal{M}}^0 \setminus \mathcal{M}^0$ (see figure 5). In both cases we ask for a C^1-surface restoration or blending. Indeed, we state the following problem:

Find a surface patch $\mathcal{M}$, such that $\tilde{\mathcal{M}} := \mathcal{M} \cup \mathcal{M}^{ext}$ minimizes the Willmore energy

$$E[\mathcal{M}] := \frac{1}{2} \int_{\mathcal{M}} h^2 \, \mathrm{d}x$$

over all C^1-surfaces $\tilde{\mathcal{M}}$ with fixed exterior surface $\mathcal{M}^{ext}$.

Here and in the following, h denotes the mean curvature of $\mathcal{M}$. The required C^1-continuity can be expressed in terms of the parameterization of the surface x (which we mostly assume to be the identity mapping) and the surface normal n. In particular we require the boundary conditions

$$\begin{aligned} x &= x^{ext}, \\ n &= n^{ext} \end{aligned} \tag{1}$$

on $\partial\mathcal{M}$, where x^{ext} is the identity on $\partial\mathcal{M}^{ext} = \partial\mathcal{M}$ and n^{ext} the corresponding surface normal. We are aiming to solve this problem based on the gradient descent with respect to the Willmore energy $E[x] = E[\mathcal{M}]$

$$\partial_t x(t) = -\mathrm{grad}_{L^2} E[x(t)], \tag{2}$$

which defines a one parameter family of surfaces $\mathcal{M}(t)$. As initial condition we consider

$$\mathcal{M}(0) = \mathcal{M}^0$$

and require the above boundary conditions (1) for all $t > 0$. We expect that $\mathcal{M}(t)$ converges to a stable critical point of the above variational problem.

The main contribution of this paper is to derive a variational formulation for the above initial boundary value problem which then can be discretized by a finite element method in a straightforward way. In fact, our aim is to discretize both, the mean curvature vector $y := h\, n$ and the surface parameterization x, using piecewise affine finite elements. The method is directly applicable to triangular meshes as they frequently appear in geometric modeling applications. No recovery of higher order differential quantities from the triangular surface meshes is required. The time discretization is semi implicit, which is of superior importance for the efficiency of the presented approach, c.f. also [7]. The discrete elliptic operator of a fourth order problem is known to be characterized by a condition number $O(h^{-4})$, where h indicates the grid size. To ensure stability of an explicit discretization we would be lead to a severe restriction of the type

$$\tau \leq Ch^4$$

for the time step size τ (cf. results presented in [29, 4]). Our semi implicit scheme allows much larger time steps. Numerical experiments show that time steps of the order of the spatial grid size are still feasible with respect to the stability of the approach.

In the restoration of flat 2D images - known as the inpainting problem - variational methods have proved to be successful tools. Methods which are related to the minimization of the total variation allow a continuation of edges from outside the destroyed

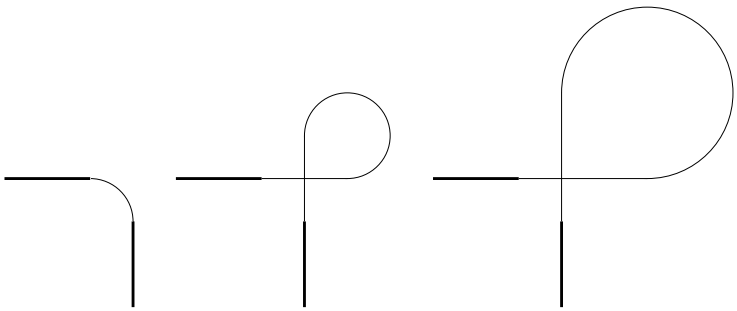

Figure 1: *Different C^1 solutions of the blending problem.*

image region into its interior. These methods lead to nonlinear second order partial differential equations with Dirichlet boundary conditions. For an overview we refer to [5]. Furthermore, fourth order methods have been presented for image inpainting problems as well [3, 2]. They prescribe gradient directions and grey values at the boundary of the inpainting domain and minimize an energy depending on directions and image intensities under these boundary constraints. One obtains a coupled system of second order partial differential equations, which is closely related to a fourth order partial differential equation. Recently, curvature based inpainting methods [4, 1] have been proposed which treat the level sets of a 2D images as Euler elastica and minimize their bending energy.

For the restoration of surfaces, second order approaches will not lead to satisfying results. In analogy to the BV minimizing approach for image inpainting we would have to ask for surface patches, which are minimal surfaces [11]. Indeed we ask for a restoration of the enclosed volume with minimal perimeter, i.e., the characteristic function minimizes the BV norm under suitable boundary conditions. This corresponds to boundary conditions for the position vector only and not for the surface normal. Hence, one cannot expect C^1-smooth surfaces.

In [25] Kobbelt and Schneider use a fourth order method to obtain smoothness of the surface at the boundary. Essentially they construct a surface of prescribed mean curvature, where the mean curvature is obtained by elliptic interpolation of the mean curvature at the boundary. Greiner [12, 13] presented a surface blending method, where in a fix point iteration parameterized patches are constructed which minimize a linearized total curvature. In the iteration one expects a successively better approximation of the actual total curvature by this linearization. Recently a method for the restoration of surfaces based on a gradient descend method for a discrete version of the Willmore energy has been presented by Yoshizawa and Belyaev [29]. This scheme uses the classical formulation of Willmore flow. Curvature quantities are computed based on certain approximation schemes. In particular the mean curvature is evaluated applying the so called umbrella operator [15]. The time discretization is explicit and hence large numbers of time steps are reported already for moderately fine discretized surfaces.

Finally, let us make some principle remarks on the formulated problem. There are geometric configurations where solutions of the above variational problem do not exist.

Indeed, for $d = 1$ and a circular segment $\mathcal{M}_{circ}$ with an opening angle α and radius r one computes a Willmore energy $E[\mathcal{M}_{circ}] = \frac{\alpha}{r}$. Thus, for two given curve segments which have to be blended we can continue these segments by straight line segments and connect them by such a circular arc. As the length of the straight line segments tends to infinity the Willmore energy of the whole blending construction tends to 0. This example is due to U. Reif. A similar construction is possible for half planes of codimension 1, whose boundaries are parallel.

In the present paper, for $d = 2$ we consider the energy density $h^2 = (\kappa_1 + \kappa_2)^2$, where κ_1 and κ_2 indicate the principle curvatures of the surface. Alternatively, one might consider the integrand $\kappa_1^2 + \kappa_2^2$. For given topological type of the minimizing surface these two approaches are equivalent due to the Gauß Bonnet theorem [28, pp. 146]. Indeed, for closed surfaces the integral over the Gauß curvature $\int_{\mathcal{M}} \kappa_1 \kappa_2$ is a topological invariant.

This consideration leads to the following view: The restoration problem can be regarded as a generalization of cubical splines for one dimensional blending problems. A cubical spline is known to minimize the L^2-norm of the second derivatives of the curve parameterization - which is a linearization of curvature - under C^1-constraints at the boundary [9].

Concerning physical modeling the minimization of the Willmore energy is closely related to the minimization of the bending energy of an elastic shell [6, 14]. An analysis concerning the structure of integrands appearing in elasticity is due to Nitsche [20]. The Willmore functional is a special case of functionals with integrands depending on the principal curvatures κ_1 and κ_2. Nitsche was able to show that integrands which are symmetric, definite and of polynomial growth of order at most two are of the form:

$$\alpha + \beta(h - h_0)^2 - \gamma k \,,$$

where α, β, γ and h_0 are constants fulfilling certain structural inequalities. Furthermore, k is Gauß curvature. Nevertheless, the physical meaning of the pure Willmore functional ($\alpha = \gamma = h_0 = 0$, $\beta = 1$) is limited. Any sphere is a minimizer and the area of Willmore surfaces cannot be bounded (see also the discussion in 1D above).

Recently, the L^2-gradient flow of the Willmore energy was considered analytically. Simonett was able to prove long time existence for surfaces close to spheres in the $C^{2,\alpha}$ topology. Kuwert and Schätzle [17] show the existence of a lower bound on the maximal time for which smooth solutions of the Willmore flow exist. In particular they analyze the concentration of the curvature. In [16, 18] they are able to prove that for surfaces of sphere type and initial energy less than or equal 8π, Willmore flow converges to a round sphere. (Note that in the present paper notation spheres have energy 8π in contrast to 4π which is the usual convention in geometry.)

The case of curves moving in space w.r.t. Willmore flow is considered by Dziuk, Kuwert and Schätzle in [8] analytically and numerically. They generalize results of Polden for planar curves [21, 22] and give a semi-implicit discretization scheme.

Notation

Let us summarize notations and conventions we use in the sequel. We consider an oriented embedded surface $\mathcal{M} \subset \mathbb{R}^3$. Usually the parameterization x is the identity on

the surface $\mathcal{M}$. The metric on $\mathcal{M}$ is simply induced by the ambient space. The corresponding area-element will be denoted by $\mathrm{d}x$. Due to the fact that bounded surfaces are considered, the induced area-element on the boundary $\partial\mathcal{M}$ is taken into account and denoted by $\mathrm{d}H^1$.

We will use the concept of tangential gradients. The tangential gradient $\underline{D}_{\mathcal{M}} u$ for a function $u \in C^1$ defined in a neighborhood of an embedded surface $\mathcal{M}$, is given by

$$\underline{D}_{\mathcal{M}} u = \nabla_{\mathbb{R}^3} u - (n \cdot \nabla_{\mathbb{R}^3} u)\, n\,,$$

where $n : \mathcal{M} \to S^2$ is the normal mapping. Here and in the following, the scalar product of two vectors $a, b \in \mathbb{R}^m$ is denoted by $a \cdot b$. The tangential gradient only depends on the values of u on $\mathcal{M}$. It is almost everywhere defined for surfaces $\mathcal{M} \in C^{0,1}$ and coincides with the classical geometric gradient $\nabla_{\mathcal{M}} u$ for embedded surfaces. The components of $\underline{D}_{\mathcal{M}} u$ are denoted by $\underline{D}_{\mathcal{M},i} u$. We also use just $\underline{D} u$ and $\underline{D}_i u$ if any misunderstanding is ruled out. In this notation, the Laplace operator on surfaces is given by:

$$\Delta_{\mathcal{M}} u = \sum_i \underline{D}_i \underline{D}_i u.$$

For surfaces of codimension 1, curvature may be expressed by the shape operator S which is – using tangential gradients – given by the 3×3-matrix $S = \underline{D}_{\mathcal{M}} n = \nabla_{\mathcal{M}} n$. The classical mean curvature then is:

$$h = \operatorname{tr}\, \nabla_{\mathcal{M}} n$$

and we have the well known identity

$$\Delta_{\mathcal{M}} x = h\, n\,.$$

The norm of the shape-operator is defined as

$$|S|^2 = \operatorname{tr}\,(S^2) = \operatorname{tr}\,(\nabla_{\mathcal{M}} n\, \nabla_{\mathcal{M}} n)\,.$$

For more details on tangential gradients we refer to [10, Chapter 16].

The Frobenius norm on the space of matrices in $\mathbb{R}^{m\times m}$ is denoted by $|A| := \sqrt{\operatorname{tr}\,(A^T A)}$, where the corresponding scalar product is

$$A : B = \operatorname{tr}\,(A^T B)\,,$$

for $A, B \in \mathbb{R}^{m\times m}$. The tensor product of two vectors is defined as the matrix $a \otimes b$ with components $(a \otimes b)_{ij} = a_i b_j$. We shall use the Einstein summation convention where it is convenient.

2 L^2 gradient of the Willmore functional

In this section we will consider time dependent embedded surfaces $\mathcal{M}(t)$ in $\mathbb{R}^3$. We usually identify the surface and its parameterization $x(t) = x(\cdot, t)$. The time dependency will be such that the surface moves w.r.t. the L^2-gradient flow of the Willmore functional:

$$E[x] = \frac{1}{2} \int_{\mathcal{M}} h^2 \, \mathrm{d}x\,. \tag{3}$$

The first variation of curvature functionals is well known. For corresponding computations and references to the literature see e.g. [28, 19, 27]. Usually, authors take into account only variations w.r.t. normal direction. Due to the fact, that $E[x]$ is a geometric functional, this is sufficient for geometric purposes. Taking into account a family of surfaces $x_\epsilon = x + \epsilon\,\varphi n$ leads to

$$\partial_\epsilon E[x_\epsilon]_{|\epsilon=0} = \int_{\mathcal{M}} -h\Delta_{\mathcal{M}}\varphi - (|S|^2 - \frac{1}{2}h^2)h\,\varphi \,\mathrm{d}x\,.$$

From the geometric character of E one derives that the velocity of the corresponding L^2-gradient flow points in normal direction. By the above representation, the classical equation for Willmore flow (2) is given by:

$$\partial_t x = (\Delta_{\mathcal{M}} h + h\,(|S|^2 - \frac{1}{2}h^2))\,n\,.$$

Nevertheless, in numerical applications one has to consider general variations. This is because in discrete weak formulations of the corresponding problems, test functions are basis functions of a finite element space. In general, those are not pointing in normal direction nor is this normal direction everywhere defined. Now we come to a formulation of the Euler-equation which is valid for general variations. For a test function $\vartheta \in C^1(\mathcal{M}, \mathbb{R}^3)$ we have

$$\langle E'[x], \vartheta\rangle = \frac{d}{d\epsilon} E[x_\epsilon]_{|\epsilon=0}\,,$$

where x_ϵ fulfills $\partial_\epsilon x_{\epsilon|\epsilon=0} = \vartheta$. The following lemma is taken from [23].

Lemma 2.1 *Let $x : \mathcal{M} \to \mathbb{R}^3$ be an immersion. For the derivative of the Willmore functional in direction ϑ we have*

$$\begin{aligned}\langle E'[x], \vartheta\rangle \quad &= \quad \int_{\mathcal{M}} \Delta_{\mathcal{M}} x \cdot [\Delta_{\mathcal{M}}\vartheta + 2n\,(\nabla_{\mathcal{M}} n : \nabla_{\mathcal{M}}\vartheta)]\,\mathrm{d}x \\ &\quad + \frac{1}{2}\int_{\mathcal{M}} |\Delta_{\mathcal{M}} x|^2\,(\nabla_{\mathcal{M}} x : \nabla_{\mathcal{M}}\vartheta)\,\mathrm{d}x\,. \qquad (4)\end{aligned}$$

The above weak form of the Euler equation for the Willmore functional does not use integration by parts at all. Especially, expressions containing boundary integrals do not appear thus far. The following section discusses a numerically well suited form of the Euler equation and the corresponding boundary terms.

3 A boundary value problem for Willmore flow

Let us first recall the basic result on integration by parts on surfaces:

Lemma 3.1 (Green's formula on surfaces) *For functions $u \in H^2(\mathcal{M})$ and $\psi \in H^1(\mathcal{M})$ on a manifold $\mathcal{M}$ with boundary the following integration by parts formula holds:*

$$\int_{\mathcal{M}} \nabla_{\mathcal{M}} u \cdot \nabla_{\mathcal{M}}\psi \,\mathrm{d}x = -\int_{\mathcal{M}} \Delta_{\mathcal{M}} u\,\psi \,\mathrm{d}x + \int_{\partial\mathcal{M}} \partial_{n^{co}} u\,\psi \,\mathrm{d}H^1\,.$$

Here n^{co} denotes the co–normal on $\partial\mathcal{M}$.

Proof: Consider a cut off function $\eta_\epsilon := \frac{1}{\epsilon}\min\{\text{dist}(x,\partial\mathcal{M}),\epsilon\}$, where $\text{dist}(\cdot,\partial\mathcal{M})$ denotes the geodesic distance from the boundary $\partial\mathcal{M}$ on $\mathcal{M}$. Now we recall the definition of the divergence operator and the Laplace Beltrami operator on manifolds, and obtain

$$\begin{aligned}\int_{\mathcal{M}} \nabla_{\mathcal{M}} u \cdot \nabla_{\mathcal{M}} \psi\, \eta_\epsilon \,\mathrm{d}x &= -\int_{\mathcal{M}} \nabla_{\mathcal{M}} u \cdot \nabla_{\mathcal{M}} \eta_\epsilon\, \psi \,\mathrm{d}x + \int_{\mathcal{M}} \nabla_{\mathcal{M}} u \cdot \nabla_{\mathcal{M}} (\psi\,\eta_\epsilon)\,\mathrm{d}x \\ &= -\int_{\mathcal{M}} \nabla_{\mathcal{M}} u \cdot \nabla_{\mathcal{M}} \eta_\epsilon\, \psi \,\mathrm{d}x - \int_{\mathcal{M}} \text{div}_{\,\mathcal{M}} \nabla_{\mathcal{M}} u\, \psi\, \eta_\epsilon \,\mathrm{d}x \\ &\xrightarrow{\epsilon\to 0} \int_{\partial\mathcal{M}} \nabla_{\mathcal{M}} u \cdot n^{co}\, \psi \,\mathrm{d}H^1 - \int_{\mathcal{M}} \Delta_{\mathcal{M}} u\, \psi \,\mathrm{d}x\end{aligned}$$

Furthermore the left hand side converges to $\int_{\mathcal{M}} \nabla_{\mathcal{M}} u \cdot \nabla_{\mathcal{M}} \psi \,\mathrm{d}x$. □

Now we are able to generalize Lemma 2 in [23] to the situation of bounded surfaces. The result is contained in the next

Proposition 3.2 *Let x be as in Lemma 2.1. For $y = \Delta_{\mathcal{M}} x$, the derivative of the Willmore functional in direction ϑ is given by:*

$$\begin{aligned}\langle E'[x],\vartheta\rangle &= \int_{\mathcal{M}} (\mathrm{Id} - 2n\otimes n)\nabla_{\mathcal{M}} y : \nabla_{\mathcal{M}}\vartheta \,\mathrm{d}x \\ &\quad + \frac{1}{2}\int_{\mathcal{M}} |y|^2 \nabla_{\mathcal{M}} x : \nabla_{\mathcal{M}}\vartheta \,\mathrm{d}x + \int_{\partial\mathcal{M}} \partial_{n^{co}}\vartheta \cdot y \,\mathrm{d}H^1 . \qquad (5)\end{aligned}$$

Proof: Due to (4), it suffices to show the identity

$$\begin{aligned}&\int_{\mathcal{M}} y\cdot[\Delta_{\mathcal{M}}\vartheta + 2n\,(\nabla_{\mathcal{M}} n : \nabla_{\mathcal{M}}\vartheta)]\,\mathrm{d}x = \\ &\int_{\mathcal{M}} \nabla_{\mathcal{M}} y : \nabla_{\mathcal{M}}\vartheta \,-2\,n_i \underline{D}_k y_i n_l \underline{D}_k \vartheta_l \,\mathrm{d}x + \int_{\partial\mathcal{M}} \partial_{n^{co}}\vartheta_i\, y_i \,\mathrm{d}H^1\end{aligned}$$

with $y = \Delta_{\mathcal{M}} x$. Let us start with considering the term

$$\begin{aligned}&2\int_{\mathcal{M}} (n\cdot y)\,\nabla_{\mathcal{M}} n : \nabla_{\mathcal{M}}\vartheta \,\mathrm{d}x \\ =\;& 2\int_{\mathcal{M}} \nabla_{\mathcal{M}}(n\cdot y\, n) : \nabla_{\mathcal{M}}\vartheta \,\mathrm{d}x - 2\int_{\mathcal{M}} \nabla_{\mathcal{M}}(n_k y_k) n_s \nabla_{\mathcal{M}}\vartheta_s \,\mathrm{d}x \\ =\;& 2\int_{\mathcal{M}} \nabla_{\mathcal{M}} y : \nabla_{\mathcal{M}}\vartheta \,\mathrm{d}x - 2\int_{\mathcal{M}} n_k n_s \nabla_{\mathcal{M}} y_k \nabla_{\mathcal{M}}\vartheta_s \,\mathrm{d}x \\ &-2\int_{\mathcal{M}} y_k \nabla_{\mathcal{M}} n_k\, n_s \nabla_{\mathcal{M}}\vartheta_s \,\mathrm{d}x \qquad (6)\end{aligned}$$

The last term in the above equation vanishes due to the symmetry of $\nabla_{\mathcal{M}} n$ and the identity $y = -hn$. Applying Lemma 3.1 componentwise we obtain

$$\int_{\mathcal{M}} y\cdot\Delta_{\mathcal{M}}\vartheta \,\mathrm{d}x = -\int_{\mathcal{M}} \nabla_{\mathcal{M}} y : \nabla_{\mathcal{M}}\vartheta \,\mathrm{d}x + \int_{\partial\mathcal{M}} \partial_{n^{co}}\vartheta\cdot y \,\mathrm{d}H^1 . \qquad (7)$$

Adding (6) and (7) gives us the desired result.

□

Now we have to keep in mind that we are interested in solving a boundary value problem with smoothness conditions at the boundary. Especially we seek for C^1-smooth solutions. Therefore, we cannot admit any test function. For smoothness at the boundary, we have to restrict to ϑ and $\partial_{n^{co}}\vartheta$ vanishing at the boundary, thus $\nabla_{\mathcal{M}}\vartheta = 0$ on $\partial\mathcal{M}$. Finally in the class of admissible test functions $\{\vartheta \in C^1(\mathcal{M}) : \vartheta_{|\partial\mathcal{M}} = 0, \partial_{n^{co}}\vartheta|_{\partial\mathcal{M}} = 0\}$, the first variation of E is:

$$\begin{aligned}\langle E'[x], \vartheta\rangle &= \int_{\mathcal{M}} (\mathrm{Id} - 2n\otimes n)\nabla_{\mathcal{M}} y : \nabla_{\mathcal{M}}\vartheta \,\mathrm{d}x \\ &\quad + \frac{1}{2}\int_{\mathcal{M}} |y|^2 \nabla_{\mathcal{M}} x : \nabla_{\mathcal{M}}\vartheta \,\mathrm{d}x\,. \end{aligned} \tag{8}$$

Based on the above formula for the variation of the Willmore functional under variations of the surface, we are now able to rewrite the Willmore flow as a system of equations for the parameterization x and the mean curvature vector y.

In particular, we consider the L^2 gradient flow for the Willmore energy with initial condition and Dirichlet boundary conditions. Thus seek solutions of the evolution problem

$$\begin{aligned} \partial_t x &= \left(\Delta_{\mathcal{M}} h + h\left(|S|^2 - \tfrac{1}{2}h^2\right)\right) n && \text{on } (0,T]\times\mathcal{M}\,, \\ x &= x^{ext} && \text{on } (0,T]\times\partial\mathcal{M}\,, \\ n &= n^{ext} && \text{on } (0,T]\times\partial\mathcal{M}\,, \\ \mathcal{M}(0) &= \mathcal{M}^0\,. \end{aligned} \tag{9}$$

Instead of the normal n on the boundary we can also prescribe the outer co–normal field n^{co} on $\partial\mathcal{M}$. Then applying equation (8) and Lemma 3.1, the corresponding weak formulation is given by:

Find a family of bounded surfaces $\{\mathcal{M}(t)\}$ with $x(t)$ indicating the parameterization of $\mathcal{M}(t)$ over itself and an accompanying vector field $y(t)$ on $\mathcal{M}(t)$, such that

$$\begin{aligned} \int_{\mathcal{M}} \partial_t x\,\vartheta \,\mathrm{d}x &+ \int_{\mathcal{M}} (\mathrm{Id} - 2\,n\otimes n)\nabla_{\mathcal{M}} y : \nabla_{\mathcal{M}}\vartheta \,\mathrm{d}x \\ &= -\int_{\mathcal{M}} \frac{|y|^2}{2}\nabla_{\mathcal{M}} x : \nabla_{\mathcal{M}}\vartheta \,\mathrm{d}x \end{aligned} \tag{10}$$

$$-\int_{\mathcal{M}} \nabla_{\mathcal{M}} x : \nabla_{\mathcal{M}}\psi \,\mathrm{d}x + \int_{\partial\mathcal{M}} n^{co}\psi \,\mathrm{d}H^1 = \int_{\mathcal{M}} y\,\psi \,\mathrm{d}x\,, \tag{11}$$

for all $\vartheta \in H_0^1(\mathcal{M})$, $\psi \in H^1(\mathcal{M})$, and for almost every $t \in (0,T]$. Furthermore we assume $x = x^{\partial}$ on $(0,T]\times\partial\mathcal{M}$ and $\mathcal{M}(0) = \mathcal{M}^0$.

Lemma 3.3 (strong solutions of the initial boundary value problem) *Suppose $\mathcal{M}(t)$ is a C^2-surface for almost every $t \in (0,T]$. Then a solution of the variational problem (10), (11) is a solution of the classical problem with the above Dirichlet boundary conditions (9).*

Proof: In the second equation we apply Lemma 3.1 for $u = x$ and get

$$\int_{\partial\mathcal{M}} (\partial_{n^{co}} x - n^{co})\, \psi \, \mathrm{d}H^1 = \int_{\mathcal{M}} (y + \Delta_{\mathcal{M}} x)\, \psi \, \mathrm{d}x \tag{12}$$

for all $\psi \in H^1(\mathcal{M})$. If we restrict to test functions $\psi \in H_0^1(\mathcal{M})$ we obtain by the fundamental lemma that $y = \Delta_{\mathcal{M}} x$ almost everywhere. Hence the right hand side of (1) vanishes and again by the fundamental lemma - now with respect to the integration over $\partial\mathcal{M}$ - we finally achieve the required boundary condition $\partial_{n^{co}} x = n^{co}$ in an H^1-dimensional sense on $\partial\mathcal{M}$.

Now (9) follows immediately for test functions in the set of admissible test functions $\{\vartheta \in C^1(\mathcal{M}) : \vartheta_{|\partial\mathcal{M}} = 0,\, \partial_{n^{co}} \vartheta_{|\partial\mathcal{M}} = 0\}$.

□

Let us remark that the boundary condition $\partial_{n^{co}} x = n^{co}$ is coded solely in the second equation of this mixed formulation and that the closure of $\{\vartheta \in C^1(\mathcal{M}) : \vartheta_{|\partial\mathcal{M}} = 0,\, \partial_{n^{co}} \vartheta_{|\partial\mathcal{M}} = 0\}$ w.r.t. the $H^1(\mathcal{M})$ norm is $H_0^1(\mathcal{M})$.

4 Finite element discretization

In this section we will discuss two different numerical schemes for Willmore flow with boundary conditions. Thereby, already in the set up of the discrete problem we will consider the application to surface restoration. As in the continuous setting the resulting discrete method is a generalization of the scheme presented in [23] to problems with Dirichlet boundary conditions. Suppose $\tilde{\mathcal{M}}_h^0$ is a given triangular surface. Here h indicates the - in general spatially varying - grid size of the triangulation. Let us consider a subset $\mathcal{M}_h^0 \subset \tilde{\mathcal{M}}_h^0$ consisting of a subset of triangles. We ask for a family of discrete surfaces $\mathcal{M}_h = \mathcal{M}_h(t)$ topologically identical to $\mathcal{M}_h^0$ with $\mathcal{M}_h(0) = \mathcal{M}_h^0$ which obey a discrete Willmore flow under prescribed discrete boundary conditions. Analogous to the continuous setting $\mathcal{M}_h^{ext}$ denotes the outer surfaces $\tilde{\mathcal{M}}_h^0 \setminus \mathcal{M}_h^0$, which is supposed to be fixed in time. The two methods to be presented will differ with respect to the actual handling of the boundary condition for the surface normals.

We have to take care of the continuous boundary condition $\nabla_{\mathcal{M}} \vartheta_{|\partial\mathcal{M}} = 0$. In a discrete setting, we will achieve this either by prescribing the co-normal on the boundary (**variant I** below) or by considering a whole boundary layer instead of the boundary $\partial\mathcal{M}_h^0$. This layer consists of all triangles T in $\tilde{\mathcal{M}}_h^0 \setminus \mathcal{M}_h^0$ with $T \cap \partial\mathcal{M}_h^0 \neq \emptyset$. In this sense, we take into account an inner boundary $\partial\mathcal{M}_h^0$ and an outer boundary defined by the layer. Fixing inner and outer boundary for the position vector means obviously fixing the normal on triangles of the boundary layer (**variant II** below).

In both cases we have found a setting such that smoothness may be obtained also in a discrete sense. Nevertheless, in our implementation, the outer boundary does not appear explicitly as will become clear below.

Now, let us introduce some further notation. The set of the nodes of $\mathcal{M}_h$ is denoted by $\mathcal{N}_h$ and splits into interior $\mathcal{N}_h^{int}$ and boundary nodes $\mathcal{N}_h^{\partial}$, i.e., $\mathcal{N}_h = \mathcal{N}_h^{int} \cup \mathcal{N}_h^{\partial}$. We denote the corresponding index sets by I and I^{int} respectively. Furthermore, let $\tilde{\mathcal{V}}_h$ indicate the space of continuous, piecewise affine functions on the timedependent

surfaces $\tilde{\mathcal{M}}_h(t)$ and $\mathcal{V}_h$ the subset which vanishes on all nodes except those in $\mathcal{N}_h$. Suppose $\Psi_i \in \mathcal{V}_h$ is the nodal basis function corresponding to the node $X_i \in \mathcal{N}_h$. Correspondingly $\mathcal{V}_h^{int}$ is a further subset with support on $\mathcal{M}_h(t)$, hence in addition vanishing on the boundary nodes $\mathcal{N}_h^{\partial}$.

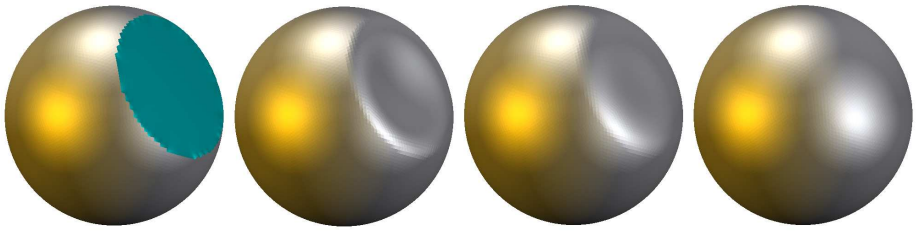

Figure 2: *Different timesteps of Willmore flow for an initial spherical surface $\tilde{\mathcal{M}}_0$ with a flattened part $\mathcal{M}^0$ (marked in blue on the left).*

To distinguish discrete quantities from their continuous counterparts wherever possible we will use uppercase letters for discrete and lowercase letters for continuous quantities, respectively. Let us denote by $R\,U$ the restriction of $U \in \mathcal{V}_h$ to a function $RU \in \mathcal{V}_h^{int}$ and by $E\,U$ the extension of a function $U \in \mathcal{V}_h^{int}$ - on $\partial\mathcal{M}_h(t)$ by 0 - onto $\mathcal{V}_h$. By $\mathbf{E}$, $\mathbf{R}$ we denote the matrices corresponding to the extension and the restriction operators E and R, respectively. In particular $\mathbf{E} \in \mathbb{R}^{\sharp I^{int},\sharp I}$ and $\mathbf{R} \in \mathbb{R}^{\sharp I,\sharp I^{int}}$. Functions U in $\mathcal{V}_h$ or $\mathcal{V}_h^{int}$ can be represented by nodal vectors $\bar{U}$ in $\mathbb{R}^{\sharp I}$ or $\mathbb{R}^{\sharp I^{int}}$ respectively, where $\bar{U} = (\bar{U}_j)_{j\in J}$ is a vector with components $\bar{U}_j$ for every j in an index set J. In analogy we denote by $A \in \mathbb{R}^{(\sharp J)^2}$ a quadratic matrix $A = (A_{jk})_{j,k\in J}$ over the index set J.

Hence, $X(t)$ will be the parameterization of $\mathcal{M}_h(t)$, in particular $X(t)$ is in each component an affine linear function on the triangles of $\mathcal{M}_h(t)$. Hence, we get $X(t) \in (\mathcal{V}_h)^3$.

Let $\bar{X}^{ext}+\mathbf{E}\,\bar{X}$ be the corresponding nodal vector in $\mathbb{R}^{3\sharp I}$. Here $\bar{X}(t) = (\bar{X}_i(t))_{i\in I^{int}} \in \mathbb{R}^{3\sharp I^{int}}$ is the vector of node position for all interior nodes and $\bar{X}^{ext} \in \mathbb{R}^{3\sharp I}$ is the position vector for the boundary nodes with 0 entries for all interior nodes. By $\bar{X}_i(t)$ we denote the position of the i th node from $\mathcal{N}_h^{int}$ in $\mathbb{R}^3$. The representation of $R\,X(t)$ in the basis $\{\Psi_i\}_{i\in I^{int}}$ is given by

$$R\,X(t) = \sum_{i\in I^{int}} \bar{X}_i(t)\Psi_i\,.$$

We have the same representation for the discrete counterpart $\bar{Y}_i(t)$ of $y(t) = \Delta_{\mathcal{M}(t)}x(t)$ on $\mathcal{M}_h(t)$:

$$Y(t) = \sum_{i\in I} \bar{Y}_i(t)\Psi_i\,.$$

In the nodal vectors, we use the following ordering: We build blocks for each of the three coordinate components and in each block we list the corresponding components of the nodal vectors for all nodes.

Now, we are able to formulate the discrete Willmore flow following [23] for the case with boundary. We will present two variants of the numerical scheme.

The first explicitly encodes the co-normal - where as the second is an alternative which takes advantage of the fact that we have an outer surface $\mathcal{M}_h^{ext}$ on which close to $\partial\mathcal{M}_h(t)$ reliable normals are supposed to be given.

Variant I. Let T be any triangle with at least one edge on $\partial\mathcal{M}_h(t)$ and denote by N^{co} the co–normal on that edge lying in the plane of T and pointing outwards. We can regard the set of all those co–normals N^{co} as a fixed function on $\partial\mathcal{M}_h(t)$ being piecewise constant on the edges. The normal on each triangle is denoted by $N(t)$ in the following. Then we ask for a family of parametrizations $X(t) \in \tilde{\mathcal{V}}_h$ of triangular surfaces $\tilde{\mathcal{M}}_h(t)$ with $\tilde{\mathcal{M}}_h(0) = \tilde{\mathcal{M}}_h^0$ and $X(t)$ being fixed on $\mathcal{M}_h^{ext}$, and a family of vector valued functions $Y(t) \in (\mathcal{V}_h)^3$ such that

$$\begin{aligned}
&\int\limits_{\mathcal{M}_h(t)} \partial_t R X(t)\,\Theta \,\mathrm{d}x - \int\limits_{\mathcal{M}_h(t)} \nabla_{\mathcal{M}_h(t)} Y(t) : \nabla_{\mathcal{M}_h(t)}\Theta \,\mathrm{d}x \\
&= -2 \int\limits_{\mathcal{M}_h(t)} (\mathrm{Id} - N(t)\otimes N(t))\nabla_{\mathcal{M}_h(t)} Y(t) : \nabla_{\mathcal{M}_h(t)}\Theta \,\mathrm{d}x \\
&\quad - \int\limits_{\mathcal{M}_h(t)} \frac{|Y(t)|^2}{2} \nabla_{\mathcal{M}_h(t)} X(t) : \nabla_{\mathcal{M}_h(t)}\Theta \,\mathrm{d}x
\end{aligned}$$

for all $\Theta \in (\mathcal{V}_h^{int})^3$ and $t > 0$. Simultaneously, the relation

$$\int\limits_{\mathcal{M}_h(t)} Y(t)\,\Psi \,\mathrm{d}x = -\int\limits_{\mathcal{M}_h(t)} \nabla_{\mathcal{M}_h(t)} X(t) : \nabla_{\mathcal{M}_h(t)}\Psi \,\mathrm{d}x + \int\limits_{\partial\mathcal{M}_h} N^{co}\,\Psi \,\mathrm{d}H^1\,,$$

holds for all $\Psi \in (\mathcal{V}_h)^3$ and all $t > 0$. In the above system, $N(t)$ denotes the piecewise constant normal vector on $\mathcal{M}_h(t)$.

We obtain a system of ordinary differential equations on the space $\mathbb{R}^m$ with $m = 3\,\sharp I^{int}$. The degrees of freedom are the position vectors $\bar{X}_i \in \mathbb{R}^3$ for all nodes in $\mathcal{N}_h^{int}$ and coupled with them in addition the "discrete mean curvature" vectors $\bar{Y} \in \mathbb{R}^{3\sharp\mathcal{I}}$ for all nodes in $\mathcal{N}_h$. We can rewrite this problem in matrix formulation as follows:

Let us define a nonlinear $\sharp I \times \sharp I$ stiffness matrix

$$L[\omega] \quad := \quad \left(\int\limits_{\mathcal{M}_h} \omega\, \nabla\Psi_i \cdot \nabla\Psi_j \,\mathrm{d}x \right)_{i,j\in I}$$

on a given discrete surface $\mathcal{M}_h$ and the corresponding linear stiffness matrix $L := L[1]$. Furthermore, we denote by M the lumped mass matrix [26], i.e., $M_{ij} := \int_{\mathcal{M}_h} \mathcal{I}_h(\Psi_i\,\Psi_j)$ for $i, j \in I$, where $\mathcal{I}_h$ is the affine, Lagrange interpolation operator on $\mathcal{M}_h$. In addition, we define the mass matrix $M_0 \in \mathbb{R}^{\sharp I^{int},\sharp I^{int}}$ via restriction

$M_0 := \mathbf{R}M\mathbf{E}$. From these matrixes, we build block matrixes

$$\mathbf{M} = \begin{pmatrix} M & & \\ & M & \\ & & M \end{pmatrix}, \quad \mathbf{L}[\omega] = \begin{pmatrix} L[\omega_{11}] & L[\omega_{12}] & L[\omega_{13}] \\ L[\omega_{21}] & L[\omega_{22}] & L[\omega_{23}] \\ L[\omega_{31}] & L[\omega_{32}] & L[\omega_{33}] \end{pmatrix},$$

where $\omega = (\omega_{ij})_{i,j=1,2,3}$ is a matrix valued weight in $\mathbb{R}^{3,3}$ and analogously we define $\mathbf{M}_0$. The subscript indicates that this matrix is associated to the space $\mathcal{V}_h^{int}$. For a scalar weight ω we denote $\mathbf{L}[\omega] = \mathbf{L}[\omega \mathrm{Id}]$. Furthermore we use the obvious notation $\mathbf{L} = \mathbf{L}[\mathrm{Id}]$. Finally, suppose

$$\bar{N}^{co} := \left(\int_{\partial \mathcal{M}_h} N^{co} \Psi_i \, \mathrm{d}H^1 \right)_{i \in I}$$

is the vector in $\mathbb{R}^{3\sharp I}$ representing the right hand side in the second equation. Thus, we obtain

$$\begin{aligned} \mathbf{M}_0 \, \partial_t \bar{X} - \mathbf{RL} \, \bar{Y} &= -2 \, \mathbf{RL}(\mathrm{Id} - N \otimes N)\bar{Y} - \mathbf{RL}[\frac{|Y|^2}{2}](\mathbf{E}\bar{X} + \bar{X}^{ext}) \\ \bar{Y} &= -\mathbf{M}^{-1} \left(\mathbf{L}(\mathbf{E}\bar{X} + \bar{X}^{ext}) - \bar{N}^{co} \right). \end{aligned}$$

Now we introduce a semiimplicit time discretization. Hence, we replace the time derivative by a difference quotient $\frac{1}{\tau}(\bar{X}^{k+1} - \bar{X}^k)$ where τ is the time step and $(\bar{X}^k)_{k=0,\cdots} \subset \mathbb{R}^{3\sharp I^{int}}$ the sequence of nodal vectors for each time step. Any $\bar{X}^k$ describes a surface $\mathcal{M}_h^k$, which we expect to approximate $\mathcal{M}_h(\tau k)$. Finally, we obtain the following fully discrete problem:

Given $X^0 \in \mathbb{R}^{3\sharp I^{int}}$ find a sequence $(\bar{X}^k)_{k=1,\cdots} \subset \mathbb{R}^{3\sharp I^{int}}$ such that

$$\begin{aligned} &(\mathbf{M}_0 + \tau \mathbf{RLM}^{-1}\mathbf{LE} + \tau \mathbf{RL}[\frac{|Y^k|^2}{2}]\mathbf{E})\bar{X}^{k+1} \\ &\qquad = \tau \bar{F}^k + \mathbf{M}_0 \bar{X}^k - \tau \mathbf{RLM}^{-1}(\mathbf{L}\bar{X}^{ext} - \bar{N}^{co}) \end{aligned}$$

where

$$\begin{aligned} \bar{F}^k &= 2 \, \mathbf{RL}(\mathrm{Id} - N^k \otimes N^k)\mathbf{M}^{-1}(\mathbf{L}(\bar{\mathbf{E}}X^k + \bar{X}^{ext}) - \bar{N}^{co}) \\ &\quad -\mathbf{RL}[\frac{|Y^k|^2}{2}]\bar{X}^{ext}. \end{aligned}$$

In the above relations, N^k is the piecewise constant normal mapping of the surface $\mathcal{M}_h^k$.

Let us emphasize that the mass and stiffness matrices depend on a discrete surface $\mathcal{M}_h$. Here, in each time step we always consider the matrices computed for the old surface, in particular

$$\mathbf{M} = \mathbf{M}[\mathcal{M}_h^k], \quad \mathbf{L}[\omega] = \mathbf{L}[\mathcal{M}_h^k][\omega].$$

The same holds true for the weights in the originally nonlinear stiffness matrix. Hence we end up with a linear system of equations to be solved in each time step.

Let us remark, that in the above scheme we have implicitly introduced a sequence of fully discrete mean curvature vectors $(\bar{Y}^k)_{k=0,\cdots} \subset \mathbb{R}^{3\sharp I}$, with

$$\bar{Y}^{k+1} = -\mathbf{M}^{-1}\mathbf{L}(\mathbf{E}\bar{X}^{k+1} + \bar{X}^{ext}) + \mathbf{M}^{-1}\bar{N}^{co}\,,$$

where $\mathbf{M}$ and $\mathbf{L}$ – as pointed out above – depend on the surface $\mathcal{M}_h^k$.

Figure 3: *Initial (top) and restored surface (bottom) of a venus head dataset from two different views. The areas of the surface to be restored are color coded.*

Variant II. Now we proceed with a second variant for the implementation of boundary conditions. In particular, they are not encoded as Neumann data but explicitly incorporated in the discrete spaces. Basically we skip the integrals over the boundary $\partial\mathcal{M}_h$ in the above equations and exchange the integration domain, replacing

$\mathcal{M}_h$ by $\tilde{\mathcal{M}}_h$. Hence, we obtain that

$$\int\limits_{\tilde{\mathcal{M}}_h(t)} Y(t) : \Psi \, \mathrm{d}x = \int\limits_{\tilde{\mathcal{M}}_h(t)} \nabla_{\mathcal{M}_h(t)} X(t) : \nabla_{\mathcal{M}_h(t)} \Psi \, \mathrm{d}x \,,$$

holds for all $\Psi \in (\mathcal{V}_h)^3$ and all $t > 0$.

Figure 4: *Comparison of variant I (bottom) and variant II (top) of the discretization. We show the initial surfaces on the left (above with a color coded surface patch $\mathcal{M}^0$), intermediate timesteps in the middle and the restored surfaces on the right. Both variants obviously lead to very similar results.*

This simple modification ensures that in the second equation the discrete surface normals on the one ring of triangles around $\mathcal{M}_h$ are incorporated in the computation of the discrete mean curvature vector instead of explicitly coding the co-normal on the right hand side of the equation.

As in the first variant above, we can discretize this in time and end up with a sequence of linear problems to be solved in each step. We denote by $\tilde{\mathbf{M}}$ and $\tilde{\mathbf{L}}$ the mass and stiffness matrices corresponding to the integration domain $\tilde{\mathcal{M}}_h$ instead of $\mathcal{M}_h$ and obtain

$$\begin{aligned}(\mathbf{M}_0 + \tau \mathbf{R}\mathbf{L}\tilde{\mathbf{M}}^{-1}\tilde{\mathbf{L}}\mathbf{E} + \tau \mathbf{R}\mathbf{L}[\frac{|Y^k|^2}{2}]\mathbf{E})\bar{X}^{k+1} \\ = \tau \bar{F}^k + \mathbf{M}_0 \bar{X}^k - \tau \mathbf{R}\mathbf{L}\tilde{\mathbf{M}}^{-1}\tilde{\mathbf{L}}\bar{X}^{ext} \,,\end{aligned}$$

$$\bar{F}^k \quad = \quad 2\,\mathbf{R}\mathbf{L}(\mathrm{Id} - N^k \otimes N^k)\tilde{\mathbf{M}}^{-1}(\tilde{\mathbf{L}}(\bar{\mathbf{E}}X^k + \bar{X}^{ext}) - \mathbf{R}\mathbf{L}[\frac{|Y^k|^2}{2}]\bar{X}^{ext} \,.$$

Solving the system of linear equations:

The above equations are solved by a BiCG-method. Our experiments show that also a simple CG-algorithm works well.

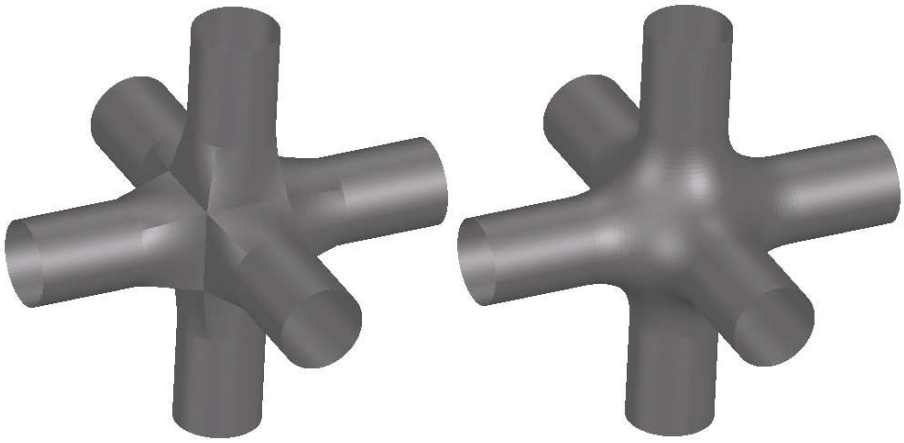

Figure 5: *In this blending problem we consider a higher genus topology. The boundary condition is determined by 6 cylinders. On the left the initial surface is shown. On the right we see the result of the Willmore-flow with C^1 boundary condition on circles around the cylinders.*

5 Applications in surface restoration

In the following section, we will discuss the application of Willmore flow to surface restoration. Let us start with an artificial test problem. In figure 2, we consider a sphere, which is flat in a geodesic circle. It is a well known fact, that spheres are (the only) minimizers of the Willmore energy [28, Thm. 7.2.2]. Therefore we expect that the application of our algorithm is able to reconstruct the sphere. We apply **variant II** (see section 4) to the (inner) flat part of the surface with the boundary conditions given by the outer sphere part. Indeed, we observe that the complete sphere is obtained within the evolution process.

Now we come to a real world restoration problem. We reconstruct damaged regions of a venus sculpture. The color coded domains of the surface in figure 3 are replaced by the corresponding Willmore surfaces with boundary conditions given by the outer surface. The boundary information of the surface X and the normal N taken from the outer surface obviously ensure smoothness of the restored surfaces.

Let us compare the two variants given in section 4(see figure 4). The upper row shows the evolution results for boundary conditions explicitly encoded in the considered spaces without Neumann conditions (**variant II**). The lower row shows the corresponding time steps using **variant I** to treat boundary values. From an application

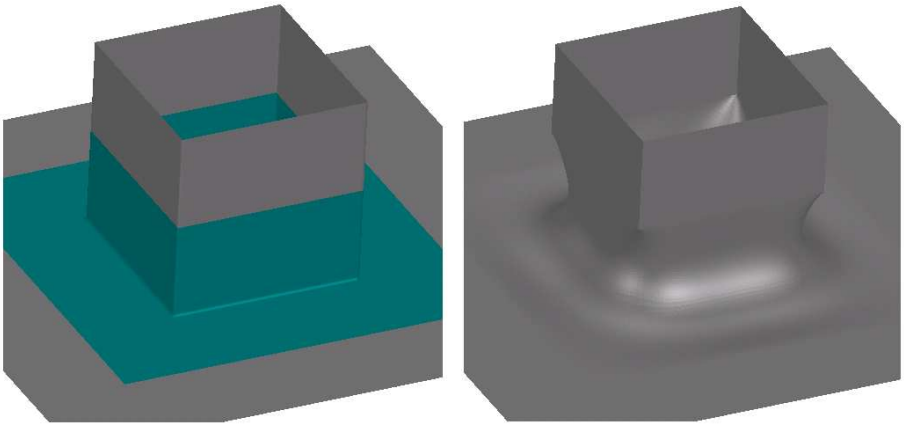

Figure 6: *Initial surface and experimental limit surface of Willmore flow with prescribed normal on the boundary. Singularities develop at the corner points on the boundary of the evolving green surface* $\mathcal{M}^0$.

oriented point of view, the quality of the results is identical. They differ slightly in the corresponding parameterization. In general one will prefer **variant II** because it is easier to implement. Nevertheless, especially w.r.t. surface modeling it is important to have both methods at hand.

Figure 5 shows a typical blending problem. We want to connect the 6 cylinders that are visible on the left hand side. The initial blend contains non-smooth parts with edges and corners. The result of Willmore flow leads to smooth blending. Let us point out that the smoothness of the boundary seems to be crucial for obtaining smooth restoration or a smooth blending. In figure 6 we solve a blending problem with our method. The resulting blending surface, which replaces the colored initial surface part of the left hand side, contains singularities. They appear exactly at those points of the boundary, where the outer surface is not smooth.

Acknowledgments

The authors would like to thank G. Greiner, L. Kobbelt, R. Schätzle, and U. Reif for inspiring discussions and valuable hints on the topic.

References

[1] L. Ambrosio and S. Masnou. A direct variational approach to a problem arising in image reconstruction. *Interfaces Free Bound.*, 5(1):63–81, 2003.

[2] M. Bertalmio, A.L. Bertozzi, and G. Sapiro. Navier-Stokes, fluid dynamics, and image and video inpainting. *Proceedings of the International Conference on Computer Vision and Pattern Recognition, IEEE*, I:355–362, 2001.

[3] M. Bertalmio, G. Sapiro, V. Caselles, and C. Ballester. Image inpainting. In *Computer Graphics (SIGGRAPH '00 Proceedings)*, 2000.

[4] T. F. Chan, S. H. Kang, and J. Shen. Euler's elastica and curvature-based inpainting. *SIAM Appl. Math.*, 63(2):564–592, 2002.

[5] T.F. Chan and J. Shen. On the role of the bv image model in image restoration. *AMS Contemporary Mathematics.* to appear.

[6] P.G. Ciarlet. *Mathematical Elasticity, Vol III: Theory of Shells*. North-Holland, 2000.

[7] G. Dziuk. An algorithm for evolutionary surfaces. *Numer. Math.*, 58:603–611, 1991.

[8] G. Dziuk, E. Kuwert, and R. Schätzle. Evolution of elastic curves in $\mathbb{R}^n$: existence and computation. *SIAM J. Math. Anal.*, 33(5):1228–1245 (electronic), 2002.

[9] G. Farin. *Curves and surfaces for computer-aided geometric design*. Computer Science and Scientific Computing. Academic Press Inc., San Diego, CA, fourth edition, 1997.

[10] D. Gilbarg and N.S. Trudinger. *Elliptic partial differential equations of second order*. Grundlehren der Mathematischen Wissenschaften. 224. Berlin-Heidelberg-New York: Springer- Verlag, 1992.

[11] E. Giusti. *Minimal surfaces and functions of bounded variation*. Birkhäuser, 1984.

[12] G. Greiner. Variational design and fairing of spline surfaces. *Computer Graphics Forum (Proc. Eurographics '94)*, 13(3):143–154, 1994.

[13] G. Greiner, J. Loos, and W. Wesselink. Data dependent thin plate energy and its use in interactive surface modeling. *Computer Graphics Forum (Proc. Eurographics '96)*, 15(3):175–186, 1996.

[14] E. Grinspun, P. Krysl, and P. Schröder. CHARMS: A Simple Franmework for Adaptive Simulation. In *Computer Graphics (SIGGRAPH '02 Proceedings)*, 2002.

[15] L. Kobbelt, S. Campagna, J. Vorsatz, and H.-P. Seidel. Interactive multi-resolution modeling on arbitrary meshes. In *Computer Graphics (SIGGRAPH '98 Proceedings)*, pages 105–114, 1998.

[16] E. Kuwert and R. Schätzle. The Willmore flow with small initial energy. *J. Differential Geom.*, 57(3):409–441, 2001.

[17] E. Kuwert and R. Schätzle. Gradient flow for the Willmore functional. *Comm. Anal. Geom.*, 10(2):307–339, 2002.

[18] E. Kuwert and R. Schätzle. Removability of Point Singularities of Willmore Surfaces. *Preprint SFB 611, Bonn*, No. 47, 2002.

[19] Nitsche, J.C.C. Boundary value problems for variational integrals involving surfaces curvatures. *Quaterly Appl. Math.*, LI, no. 2:363–387, 1993.

[20] Nitsche, J.C.C. Periodic Surfaces that are Extremal for Energy Functionals Containing Curvature Functions. In H.T. Davis and J.C.C. Nitsche, editors, *Proc. Workshop Statistical Thermodynamics and Differential Geometry of Microstructured Materials*. IMA vol. in Math. and its Appl., Springer, 1993.

[21] A. Polden. Closed Curves of Least Total Curvature. *SFB 382 Tübingen, Preprint*, 13, 1995.

[22] A. Polden. Curves and Surfaces of Least Total Curvature and Fourth-Order Flows. *Dissertation, Universität Tübingen*, 1996.

[23] R. Rusu. An algorithm for the elastic flow of surfaces. *Preprint Mathematische Fakultät Freiburg*, 01-35, 2002.

[24] R. Schneider and L. Kobbelt. Discrete Fairing of Curves and Surfaces based on Linear Curvature Distribution. In *Curve and Surface Design: Saint-Malo*, pages 371–380, 1999.

[25] R. Schneider and L. Kobbelt. Generating fair meshes with G1 boundary conditions. In *Geometric Modeling and Processing Conference Proceedings*, 2000.

[26] V. Thomée. *Galerkin - Finite Element Methods for Parabolic Problems*. Springer, 1984.

[27] H. von der Mosel. Geometrische Variationsprobleme höherer Ordnung. *Bonner Mathematische Schriften*, 293, 1996.

[28] T.J. Willmore. *Riemannian Geometry*. Claredon Press, Oxford, 1993.

[29] S. Yoshizawa and A.G. Belyaev. Fair Triangle Mesh Generation with Discrete Elastica. In *Geometric Modeling and Processing, RIKEN, Saitama, Japan*, pages 119–123, 2002.